Targeted Disruption of the Pemphigus Vulgaris Antigen (Desmoglein 3) Gene in Mice Causes Loss of Keratinocyte Cell Adhesion with a Phenotype Similar to Pemphigus Vulgaris

Peter J. Koch,* Mỹ G. Mahoney,* Hiroyasu Ishikawa,‡ Leena Pulkkinen,‡ Jouni Uitto,‡ Leonard Shultz,§ George F. Murphy,* Diana Whitaker-Menezes,* and John R. Stanley*

*Department of Dermatology, University of Pennsylvania School of Medicine, Philadelphia, Pennsylvania 19104; ‡Department of Dermatology and Cutaneous Biology, Jefferson Medical College, Philadelphia, Pennsylvania 19107; and §The Jackson Laboratory, Bar Harbor, Maine 04609

Abstract. In patients with pemphigus vulgaris (PV), autoantibodies against desmoglein 3 (Dsg3) cause loss of cell–cell adhesion of keratinocytes in the basal and immediate suprabasal layers of stratified squamous epithelia. The pathology, at least partially, may depend on protease release from keratinocytes, but might also result from antibodies interfering with an adhesion function of Dsg3. However, a direct role of desmogleins in cell adhesion has not been shown. To test whether Dsg3 mediates adhesion, we genetically engineered mice with a targeted disruption of the *DSG3* gene. DSG3 −/− mice had no DSG3 mRNA by RNase protection assay and no Dsg3 protein by immunofluorescence (IF) and immunoblots. These mice were normal at birth, but by 8–10 d weighed less than DSG3 +/− or +/+ littermates, and at around day 18 were grossly runted. We speculated that oral lesions (typical in PV patients) might be inhibiting food intake, causing this runting. Indeed, oropharyngeal biopsies showed erosions with histology typical of PV, including suprabasilar acantholysis and "tombstoning" of basal cells. EM showed separation of desmosomes. Traumatized skin also had crusting and suprabasilar acantholysis. Runted mice showed hair loss at weaning. The runting and hair loss phenotype of DSG3 −/− mice is identical to that of a previously reported mouse mutant, balding (*bal*). Breeding indicated that *bal* is coallelic with the targeted mutation. We also showed that *bal* mice lack Dsg3 by IF, have typical PV oral lesions, and have a DSG3 gene mutation. These results demonstrate the critical importance of Dsg3 for adhesion in deep stratified squamous epithelia and suggest that pemphigus autoantibodies might interfere directly with such a function.

Desmosomes are cell–cell adhesion junctions that are found in epithelia and a small number of other tissues (for review see Schwarz et al., 1990). These junctions have two basic functions: in addition to mediating cell–cell coupling, they provide anchorage for intermediate filaments via their cytoplasmic plaque and therefore function as organizational centers for part of the cytoskeleton. Given these structural features and the abundance of desmosomes in certain tissues, especially in stratified squamous epithelia, it is assumed that desmosomes are critical in providing mechanical stability to these tissues.

Two types of transmembrane proteins, desmogleins (Dsg)[1] and desmocollins (Dsc), are constitutive components of desmosomes. Both represent small families of type 1 transmembrane glycoproteins (Dsg1, Dsg2, Dsg3; Dsc1, Dsc2, Dsc3, for nomenclature see Buxton et al., 1993) that are sequence related to the previously characterized family of calcium-dependent cell adhesion molecules, the cadherins (Koch et al., 1990, 1991*a*,*b*, 1992; Goodwin et al., 1990; Amagai et al., 1991; Collins et al., 1991; Mechanic et al., 1991; Nilles et al., 1991; Parker et al., 1991; Wheeler et al., 1991; King et al., 1993; Theis et al., 1993; Troyanovsky et al., 1993; Schäfer et al., 1994; for reviews see Koch and Franke, 1994; Schmidt et al., 1994).

The members of the desmoglein and desmocollin subfamily of desmosomal cadherins show a tissue- and cell

Please address all correspondence to John R. Stanley, Department of Dermatology, University of Pennsylvania School of Medicine, 211 CRB, 415 Curie Blvd., Philadelphia, PA 19104. Tel.: (215) 898-3240. Fax: (215) 573-2033. e-mail: jrstan@mail.med.upenn.edu

G.F. Murphy and D. Whitaker-Menezes' present address is Department of Pathology, Anatomy, and Cell Biology, Jefferson Medical College, Philadelphia, PA 19107.

1. *Abbreviations used in this paper*: aa, amino acid; Dsc, desmocollin; Dsg, desmoglein; ES, embryonic stem; neo, neomycin resistance; PV, pemphigus vulgaris; PVA, PV antigen.

type–specific expression pattern (e.g., Koch et al., 1992; Arnemann et al., 1993; Theis et al., 1993; Schäfer et al., 1994, 1996; Schmidt et al., 1994; Nuber et al., 1995, 1996; Amagai et al., 1996; North et al., 1996). Some tissues, e.g., simple epithelia, express Dsg2 and Dsc2 only. In stratified squamous epithelia, however, all three desmoglein and desmocollin isoforms are present, although the expression of some of these proteins is restricted to certain strata. In human skin, for example, Dsg1 is expressed in suprabasal cell layers, Dsg2 in the basal cell layer only, and Dsg3 in the basal as well as the immediate suprabasal cell layer (Amagai et al., 1996; Schäfer et al., 1996).

In this study we focused on the biological function of one member of the desmoglein family, Dsg3. This protein has been shown to be the antigen recognized by autoantibodies from patients with the disease pemphigus vulgaris (PV), and therefore is also referred to as PV antigen (PVA) (Amagai et al., 1991).

PV is a life-threatening, autoantibody-mediated, blistering disease of the skin and mucous membranes (Stanley, 1993*a*). Blisters in these patients result from loss of keratinocyte cell-to-cell adhesion in the basal and immediate suprabasal level of stratified squamous epithelia. The typical histology of an early lesion in PV shows detachment of the epithelium just above the basal cells, usually with a few acantholytic (detached and rounded-up) cells in the blister cavity. There is no, or minimal, inflammation in an early lesion. In addition, the basal cells may detach slightly from one another while maintaining their attachment to the basement membrane, a histologic pattern referred to as a "row of tombstones" (Lever, 1965; also shown schematically in Stanley, 1993*b*). Besides the resemblance of the individual basal cells to tombstones, this designation of the histologic appearance also reflected the dismal prognosis of the disease which, before the advent of corticosteroid therapy, was almost uniformly fatal. Without therapy, patients died because these blisters rapidly lost the superficial epithelia, resulting in large areas of erosions on mucous membranes and skin. The mucous membrane lesions prevented adequate food and fluid intake, while erosions on the skin resulted in protein and electrolyte loss as well as infection. Histology of older lesions shows erosions with inflammation (which is characteristically seen in mucous membrane or skin eroded from any cause, probably secondary to infection, colonization with microbes, and/or irritation due to loss of the barrier function) and attempts at reepithelialization.

IgG autoantibodies against the cell surface of keratinocytes of stratified squamous epithelia are present in the skin and sera of PV patients, as detected by direct and indirect immunofluorescence, respectively (Stanley, 1993*a*). These antibodies are pathogenic, i.e., they cause blister formation, as proven by several lines of evidence (for review see Stanley, 1990). In general, autoantibody titer, as determined by indirect immunofluorescence, correlates with disease activity. That is, the higher the antibody titer, the more severe the disease. Furthermore, neonatal PV has been reported in infants born to mothers with active PV. As the passively transferred maternal IgG is catabolized, the infant recovers. Similarly, PV IgG passively transferred to neonatal mice causes clinically and histologically typical blisters. Finally, normal skin in organ culture incubated with PV IgG develops typical blisters, without the addition of complement or inflammatory cells.

Screening of a keratinocyte λgt11 expression library with patient sera was used to isolate cDNA encoding PVA (Amagai et al., 1991). Analysis of the predicted amino acid sequence defined PVA as Dsg3 (Buxton et al., 1993). Antibodies raised in rabbits to recombinant Dsg3, as well as patient sera, localized it, like the other desmogleins, to desmosomes, in particular to their extracellular face (Akiyama et al., 1991; Karpati et al., 1993). Recent studies have shown that antibodies against the extracellular domain of Dsg3 can cause suprabasilar blisters in neonatal mice (Amagai et al., 1992) and that the extracellular domain of Dsg3, expressed by baculovirus in Sf9 insect cells, can adsorb out all pathogenic antibodies from PV sera (Amagai et al., 1994*a*; Memar et al., 1996). Therefore, the antibodies against Dsg3 in patient sera are pathogenic. Finally, it has recently been shown that Dsg3 mRNA and antibodies to Dsg3 in patients' sera localize in epidermis to the basal and immediate suprabasal layer, exactly where blisters occur in PV (Arnemann et al., 1993; Shimizu et al., 1995; Amagai et al., 1996).

It is unclear exactly how PV autoantibodies cause loss of cell–cell adhesion. One possibility is that Dsg3 functions in cell–cell adhesion in the deep stratified squamous epithelia, and that autoantibodies from PV patients might interfere with its adhesive function. However, several points do not support such a hypothesis. First, it has been suggested that PV autoantibodies do not directly cause loss of cell adhesion, but function through stimulating release of proteases (specifically, plasminogen activator) from keratinocytes (Schiltz et al., 1978, 1979; Farb et al., 1978; Hashimoto et al., 1983, 1989; Morioka et al., 1987; Naito et al., 1989). Furthermore, although the classical cadherins (e.g., E-cadherin, N-cadherin, P-cadherin) have been directly shown to be calcium-dependent cell adhesion molecules, the desmogleins have not. Expression of classical cadherins in transfected L cells (mouse fibroblasts) mediates calcium-dependent aggregation (Nagafuchi et al., 1987). However, experiments with desmogleins do not show similar aggregation (Kowalczyk et al., 1996) nor do studies using desmocollins (Chidgey et al., 1996). Even a chimeric molecule of the extracellular domain of Dsg3 with the cytoplasmic domain of E-cadherin, which allows for proper interaction with the actin cytoskeleton through catenins (an interaction shown to be critical for E-cadherin function), mediates only weak aggregation when expressed in L cells (Amagai et al., 1994*b*). These studies suggest that Dsg3 might mediate adhesion but only does so effectively when organized with other desmosomal molecules.

Another approach to investigate whether Dsg3 is important for adhesion of keratinocytes would be to eliminate it from desmosomes in tissue. Therefore, in this study we genetically engineered a mouse with a targeted disruption of the desmoglein 3 gene (*DSG3*). We hypothesized that if the PV autoantibodies directly interfere with an adhesion function of this molecule then such a mouse might have a phenotype resembling human disease. Our findings demonstrate that Dsg3 is critical for cell adhesion in the basal and immediate suprabasilar keratinocytes, especially in the oral mucous membrane, thereby showing a differentiation- and tissue-specific adhesion function of one of the

desmogleins. Furthermore, because the pathology of these mice strikingly resembles that of humans with PV, our findings are consistent with the idea that PV autoantibodies directly interfere with this adhesive function.

Materials and Methods

Cloning and Characterization of 129/Sv DSG3 Gene

We have previously cloned partial cDNAs corresponding to mouse Dsg3 (Ishikawa et al., 1994). To initiate the cloning of the mouse *DSG3* gene, three different cDNA probes corresponding to mouse cDNA sequences were used for screening of a mouse 129/Sv genomic λFixII library (Stratagene, La Jolla, CA) (Sambrook et al., 1989). These three cDNAs, 413, 405, and 404 bp in size, respectively, corresponded to the amino-terminal, central, and carboxyl-terminal regions of the coding sequences. (These sequence data are available from EMBL/Genbank/DDBJ under accession number U86016.) A total of nine unique genomic clones were isolated and characterized by restriction enzyme digestions and Southern analysis with synthetic oligonucleotides based on exon sequences derived from the cDNA. The endonuclease digestion products were fractionated by electrophoresis on 1% agarose gels, and the sizes were estimated by comparison with standard DNA markers (New England Biolabs, Beverly, MA). Subcloning and sequencing of the genomic DNA, in comparison with cDNA sequences, allowed identification of the intron–exon borders. The sizes of the introns in the genomic DNA were determined by direct nucleotide sequencing, estimated by generating PCR products using synthetic nucleotide primers placed on the flanking exons, or by Southern blot analysis. (These sequence data [for exon 1/intron 1/exon 2] are available from EMBL/Genbank/DDBJ under accession number U86015.)

Construction of Targeting Vector

The plasmid pPNT (Tybulewicz et al., 1991), which contains a neomycin resistance (neo) and a herpes simplex virus thymidine kinase (HSV-tk) minigene (both under the control of the phosphoglycerate kinase promoter), was used to construct the targeting vector (Fig. 1 *B*). *DSG3* gene fragments were derived from two overlapping λFixII clones, both of which contained portions of exon 1. In the targeting vector the neo-cassette is flanked by a 2.1-kb DNA fragment (5′ arm, derived from ~400 bp of the 5′ end of exon 1 and ~1.7 kb of sequences upstream of exon 1) inserted into the BamHI and EcoRI sites of pPNT and a 5-kb DNA fragment (3′ arm, derived from intron 1) inserted into the XhoI and NotI sites of pPNT. This targeting vector, through homologous recombination with the *DSG3* gene locus, is predicted to delete exon 1 coding sequences for amino acids 1–16, 164 bp upstream of this coding sequence, and ~500 bp of intron 1.

Targeting of Embryonic Stem Cells and Generation of DSG3-deficient Mice

The embryonic stem (ES) cell line RW4 (Genome Systems, St. Louis, MO) was cultured according to the recommendations of the supplier. In a typical electroporation experiment, 30 μg of the NotI-linearized targeting vector was mixed with 8×10^6 RW4 cells suspended in 10 mM Hepes in PBS, pH 7.5, and electroporated with a single pulse (960 μF, 0.22 kV) using a BioRad Gene Pulser II (Hercules, CA). Electroporated cells were grown on neomycin-resistant mouse embryonic feeder cells (MEF; Genome Systems) in selection medium containing 220 μg/ml G418 and 2 μM gancyclovir (Mansour et al., 1988) for 9 d. With procedures previously described (Ramirez-Solis et al., 1992, 1993), G418/gancyclovir-resistant ES cell clones were cultured in duplicate; one set of cultures was frozen while the duplicate set was screened by Southern analysis. In the initial Southern blot screening, BamHI-digested DNA was hybridized to the probe shown in Fig. 1 *B*. Out of 628 clones tested, one clone had undergone homologous recombination (Fig. 1 *C*). Additional Southern blot analysis with additional restriction enzymes and a probe located in the *DSG3* gene just 3′ to the homologous sequences used in the targeting vector confirmed the targeting event in this cell line (data not shown.). A neo-derived probe indicated the presence of a single copy of the neo-minigene in the recombinant ES cell clone (data not shown). The targeted ES cells were found to possess a normal male karyotype (Hogan et al., 1994) and had no detectable mycoplasma infection (Mycoplasma PCR Primer Set; Stratagene). The recombinant ES cells were injected into C57Bl/6J blastocysts. Chimeric offspring were crossed with C57Bl/6J mice. DNA from agouti offspring was prepared from tail or, if mice were killed, other organs (Hogan et al., 1994) and tested for the presence of the targeted allele by Southern blot hybridization. Mice heterozygous for the targeted mutation were intercrossed to obtain homozygous DSG3 mutants.

Southern Blots

Labeled DNA probes were synthesized using a random primer labeling kit with [^{32}P]dCTP (Prime-It Rmt; Stratagene). The blots were hybridized for 2 h at 65°C with labeled probes in "rapid hybridization buffer" (Amersham, Little Chalfont, UK). Blots were washed twice (15 min each time) in 2× SSC, 0.1% SDS at room temperature and twice (15 min each time) in 0.2× SSC, 0.1% SDS at 65°C, and then exposed to X-Omat films (Eastman Kodak Co., Rochester, NY) for autoradiography.

Genomic DNA was extracted from 1 cm of mouse tails by digesting the tails overnight at 55°C in 700 μl tail buffer containing 50 mM Tris, pH 8.0, 100 mM EDTA, 100 mM NaCl, 0.4 mg/ml proteinase K, and 1% SDS. The lysate was extracted by phenol, 1:1 phenol/choroform, and then chloroform, and DNA was precipitated with isopropanol. Genomic DNA (10–20 μg) was digested overnight with restriction enzymes and electrophoresed in 0.8% agarose gels. DNA was transferred to Nytran membranes by the alkaline transfer method according to Schleicher and Schuell (Keene, NH) and was cross-linked with 120 mJ of UV light.

RNase Protection

The following cDNAs were used to synthesize biotinylated RNA antisense and sense probes with the Biotinscript kit (Ambion, Austin, TX): B9 (338 bp of mouse Dsg3 cDNA starting from 63 bp upstream of the translation initiation site), Dsg2.mc580 (mouse desmoglein 2 cDNA, provided by Werner W. Franke, German Cancer Research Center, Heidelberg, Germany), mDsg1exon15A (mouse desmoglein 1 exon 15), and pTRI-β-actin (mouse β-actin; Ambion). Tissue lysates from the skin of 2–4-d-old pups or the tongue of adult animals were prepared (Direct Protect; Ambion). Products of the protection assay were separated in 6% Tris-borate-EDTA-urea gels (Novex, San Diego, CA), and then transferred to nylon membranes (BrightStar Plus; Ambion). Biotin-labeled RNA fragments were detected with a chemiluminescent detection system (BrightStar Biodetect; Ambion).

Antibodies

A rabbit antiserum was raised against a synthetic peptide, HQWGIEGAHPEDKEITNIC (single letter amino acid code) (amino acids 667–685 [Amagai et al., 1991]), from the "intracellular anchor" domain of Dsg3, coupled to keyhole limpet hemocyanin (Imject Activated Immunogen Conjugation Kit; Pierce Chemical Co., Rockford, IL) (Tanaka et al., 1990). The rabbit antiserum was affinity purified on the peptide (ImmunoPure Ag/Ab Immobilization Kit 2; Pierce Chemical Co.) and concentrated to 0.3 mg/ml. On immunoblots, the resulting antibody identified the 130-kD Dsg3, but not the 160-kD Dsg1 or Dsg2, extracted from mouse (Fig. 2 *C*) or human (not shown) stratified squamous epithelia. In addition, two sera from PV patients, Nos. 1172 and 1409, were used to identify Dsg3 by immunofluorescence of mouse tissue.

The anti–desmoglein 1 and 2 mouse mAb DG3.10 was generously provided by W.W. Franke. We also used mAbs against desmoplakin I + II (Biodesign, Kennebunk, ME) and plakoglobin (15F11 generously provided by M. Wheelock, University of Toledo, OH).

Anti–rabbit IgG, anti–human IgG, and anti–mouse IgG antibodies coupled to fluorescent dyes (FITC, Texas red) or enzymes (HRP) were purchased from Biosource (Camarillo, CA), Bio Rad Laboratories, and Molecular Probes (Eugene, OR).

Immunofluorescence Microscopy

Cryosections were fixed for 10 min in acetone or a 1:1 mixture of acetone/methanol at −20°C, and then washed in PBS. In some experiments, tissue samples were washed for 5 min in PBS with 1% Triton X-100 after fixation, followed by several washes in PBS. The tissue samples were incubated with the first antibody at the appropriate dilution in 1% BSA in PBS for 1 h. After washing three times for 5 min each in PBS, samples were incubated with a fluorescent dye–coupled antibody diluted in 1%

BSA/PBS for 30 min and washed as described above. Stained sections were examined and photographed with a BX60 photomicroscope (Olympus Corp., Lake Success, NY).

Western Blotting

Whole tissue extracts were prepared by homogenizing mouse tongue in lysis buffer (10 mM Tris-HCl, pH 7.4, 5 mM EDTA, 420 mM NaCl, 1% Triton X-100, 100 μg/ml leupeptin, 0.5 mM PMSF, 50 μg/ml aprotinin) on ice. The lysates were centrifuged for 10 min (4°C 16,000 *g*). The pellet was suspended in Laemmli buffer (Bio Rad Laboratories), incubated for 5 min at 100°C, and then centrifuged for 5 min at 16,000 *g*. The proteins from these supernatants were separated in 8% Tris-glycine gels (Novex) and then transferred to nitrocellulose (Trans-Blot; Bio Rad Laboratories). The membranes were incubated for 1 h in blocking buffer (5% fat-free milk powder, 1% BSA, 0.1% Tween-20 in PBS).The first antibody (diluted in blocking buffer) was incubated overnight at 4°C. The membranes were washed three times, for 15 min each, in 0.1% Tween-20/PBS, and then incubated with the secondary antibody (goat anti–mouse-HRP or goat anti–rabbit-HRP, 1:1,000 dilution in PBS/0.1% Tween-20). The membranes were washed as described above. Binding of the secondary antibody was detected with the ECL system (Amersham Corp., Arlington Heights, IL).

Histology and EM

Paraffin-embedded, microtome-sectioned tissues were stained with hematoxylin and eosin by routine methods (Lavker et al., 1991). We used routine, previously described methods to examine the ultrastructure of lesional mouse skin by transmission EM (Lavker et al., 1991).

Detection and Verification of a DSG3 Mutation in bal Mice

Information on the intron–exon organization of the mouse *DSG3* gene allowed us to develop a strategy to screen for sequence variants by heteroduplex analysis using conformation-sensitive gel electrophoresis (Ganguly et al., 1993). For heteroduplex analysis, total DNA isolated from homozygous *bal*/*bal*, heterozygous *bal*/+, or wild-type mice (+/+) was used as template for amplification of exons within DSG3. Oligonucleotide primers spanning each of the 15 exons were synthesized on the basis of intronic sequences and used to generate PCR products spanning the exons. Specifically, to amplify exon 14 containing the mutation, the following primers were used: sense, 5′-GCCATAGCATGAACTGTTAG-3′; antisense, 5′-GTTGGCTTGTCTTGTGAGTT-3′.

For PCR amplification, 250 ng of genomic DNA was used as a template in the amplification buffer containing 20 pmol of each primer, 100 nmol $MgCl_2$, 20 mmol of each nucleotide, and 2.5 U of Taq polymerase (GIBCO BRL, Gaithersburg, MD), in a total vol of 50 μl. The amplification conditions were 94°C for 5 min, followed by 35 cycles of 94°C for 45 s, 55°C for 45 s, and 72°C for 45 s. Aliquots of 5 μl of the PCR products were analyzed on 2% agarose gel electrophoresis, and 10 μl of the sample was prepared for heteroduplex analysis. The PCR products demonstrating heteroduplex formation were sequenced using an ABI automated sequencer.

Since the mutation in the *DSG3* gene did not create or abolish a restriction endonuclease site, its presence was verified by allele-specific oligonucleotide hybridization. The oligonucleotide probes used for hybridization were, for the wild-type (WT) sequence, 5′-TTGAAGGACTATGCTGCGC-3′, and, for the mutant (M) allele, 5′-TGAAGGACTTATGCTGCGC-3′. These oligomers were end labeled with [γ-^{32}P]ATP and hybridized to PCR-amplified DNAs that had been immobilized to Zetabind nylon membrane. Hybridizations were carried out in 5× SSPE, 0.5% SDS, 0.1% BSA, 0.1% polyvinyl pyrrolidone/Ficoll, at 37°C for 1 h, followed by washing in 2× SSPE, 0.1% SDS at 58°C. Radioactive oligomer DNA hybrids were visualized by autoradiography on exposure to x-ray film.

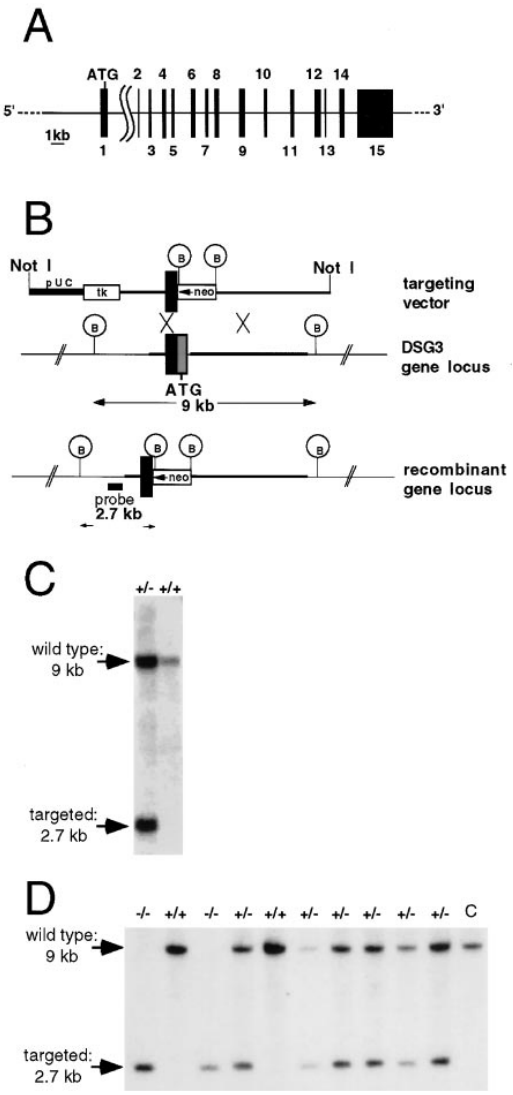

Figure 1. Targeting strategy and Southern blot confirmation of targeted alleles. (*A*) Intron–exon organization of the mouse *DSG3* gene. The exons (*vertical blocks*) and introns (*horizontal lines*) are drawn to scale, with the exception of intron 1 that is >6 kb in size. (*B*) Targeting strategy. Vertical box indicates exon 1 (lighter shading indicates part of exon 1 that is deleted in targeting strategy). *neo*, neomycin-resistance cassette; *tk*, herpes thymidine kinase cassette; *B*, BamHI sites; *NotI*, restriction site used to linearize vector; (*bold horizontal lines*) portions of the *DSG3* gene that were used in targeting vector; (*thickest horizontal line*) pUC vector sequences. Probe indicated was used in Southern blots described below. (*C*) Southern blot of DNA from wild type (+/+) and targeted (+/−) ES cell clones. DNA was digested with BamHI. Targeted allele shows a 2.7-kb band; wild-type allele shows a 9-kb band. (*D*) Southern blot of tail DNA from pups of DSG3 +/− × DSG3 +/− mating. −/−, both DSG3 alleles are targeted, resulting in only a 2.7-kb band. +/− animals show both a recombinant (2.7 kb) and wild-type (9 kb) allele, whereas +/+ animals only show a wild-type allele. Lane *C* shows control ES cell DNA.

Results

Cloning of the 129/Sv Mouse DSG3 Gene

To obtain homologous DNA sequences to target the *DSG3* gene in embryonic stem cells derived from 129/Sv mice, we cloned the gene from a 129/Sv λFixII genomic library and determined the intron–exon structure, which revealed 15 exons spanning ~25 kb of DNA (Fig. 1 *A*). The smallest exon (13) was 64 bp in size, while the last exon (15) consisted of 3,677 bp, including a segment corresponding to the 3′ untranslated sequence ending at the

polyadenylation signal. Exon 1 contained the putative translation initiation codon, ATG, as well as an upstream 5′ untranslated region.

Generation of Mice with a Targeted Disruption of the DSG3 Gene

The strategy underlying the experiments described below was to delete the coding sequence from the first exon of the *DSG3* gene, thereby functionally inactivating the gene.

We constructed a targeting vector to delete, by homologous recombination, about one-third of the 3′ end of exon 1 from one DSG3 allele in mouse 129/Sv ES cells (Fig. 1 *B*) (Horie et al., 1994; Thomas et al., 1992; Zhang et al., 1994). This part of exon 1 was replaced by a neo-cassette in the recombinant locus. The deleted part of exon 1 encodes the first 16 amino acids (aa) of the Dsg3 signal peptide and 164 bp upstream of this coding sequence (see above and Ishikawa et al., 1994). The next methionine in the aa sequence is located at position 177 (encoded by exon 6) in the second extracellular domain (EC2) of Dsg3 (Ishikawa et al., 1994; Amagai et al., 1991). Therefore, even if the neo-cassette would be spliced out of a primary transcript generated at a targeted gene locus, the resulting mRNA would encode a truncated polypeptide lacking signal sequences necessary for insertion into the cell membrane. Furthermore, the first extracellular domain of Dsg3 (EC1; Amagai et al., 1991) would be missing in this polypeptide. Although the specific function of EC1 in desmogleins is unknown, it has been shown for other cadherins (e.g., E-cadherin) that this domain of the protein is crucial for homophilic interactions (Nose et al., 1990; Blaschuk et al., 1990).

An ES clone with a targeted allele (Fig. 1 *C*) was injected into C57Bl/6J blastocysts and seven male chimeras were generated, three of which showed germline transmission of the ES cell genome as determined by the agouti coat color of offspring from chimera × C57Bl/6J breedings. As expected, Southern blot analysis revealed that ~50% of the agouti animals were heterozygous (+/−) for the targeted mutation. The DSG3+/− animals were healthy and indistinguishable from wild-type (+/+) littermates. Heterozygous mice (F1 generation) were then intercrossed to produce offspring homozygous (−/−) for the targeted allele. 132 pups derived from these intercrosses were genotyped (example in Fig. 1 *D*). Of those, 23% were +/+, 54% +/−, and 23% −/−, indicating inheritance of the targeted mutation according to Mendel's laws with no indication of significant embryonic lethality of the homozygous state. The litter size in the F2 generation was normal, and, at birth, +/+, +/−, or −/− animals could not be distinguished by visual inspection.

Taken together, these findings indicated that the targeted mutation did not significantly interfere with prenatal development. Furthermore, so far one male and one female homozygous mutant mouse were able to breed, demonstrating fertility of the mutants.

Mice Homozygous for the Targeted Mutation Do Not Synthesize Dsg3

To demonstrate that the gene targeting resulted in a functional null mutation, we studied the Dsg3 mRNA expression and protein synthesis in pups derived from intercrosses between +/− animals. Dsg3 mRNA was absent in −/− animals, whereas the mRNA was detected in +/+ and +/− animals, as determined by an RNase protection assay. (Fig. 2 *A*). The levels of Dsg1 and Dsg2 mRNA expression were not affected by the targeted mutation and were similar in +/+, +/−, and −/− mice (data not shown). Immunofluorescence microscopy on tongue epithelium using antibodies against extracellular or cytoplasmic epitopes of Dsg3 indicated the absence of the protein in −/− mutants (Fig. 2 *B*). Control antibodies against other desmogleins (e.g., mAb 3.10 that recognizes Dsg1 and Dsg2) (Fig. 2 *B*), as well as antibodies against the desmosomal plaque proteins plakoglobin (Fig. 2 *B*) or desmoplakin (not shown), showed no difference in the staining patterns in samples derived from +/+, +/−, and −/− mice. Furthermore, Western blot analysis of tongue extracts from −/− mutants demonstrated the absence of the Dsg3 polypeptide but the presence of Dsg1 and Dsg2, as indicated by mAb 3.10 (Fig. 2 *C*).

These data indicate that the targeted mutation indeed represented a functional null mutation.

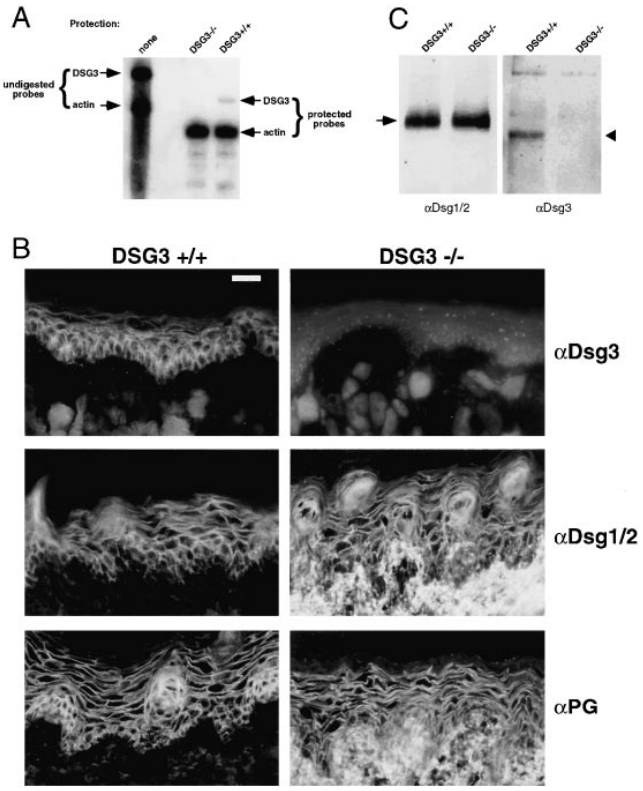

Figure 2. Lack of Dsg3 RNA and protein in homozygous targeted mice. (*A*) RNase protection assay of tongue lysates from wild type (+/+) and targeted (−/−) mice. (*B*) Immunofluorescence of tongue from wild-type and targeted mice shows absence of Dsg3 from −/− mice, but presence of Dsg 1 and 2 (*Dsg1/2*, identified by mAb DG3.10), and plakoglobin. The submucosa of −/− mice shows increased nonspecific fluorescence probably as a result of inflammation. (*C*) Western blot of tongue lysates. Dsg3 is absent in −/− mice (*arrowhead*), but Dsg1 and 2 are present (*arrow*) to the same degree as in +/+ mice. Bar, 25 μm.

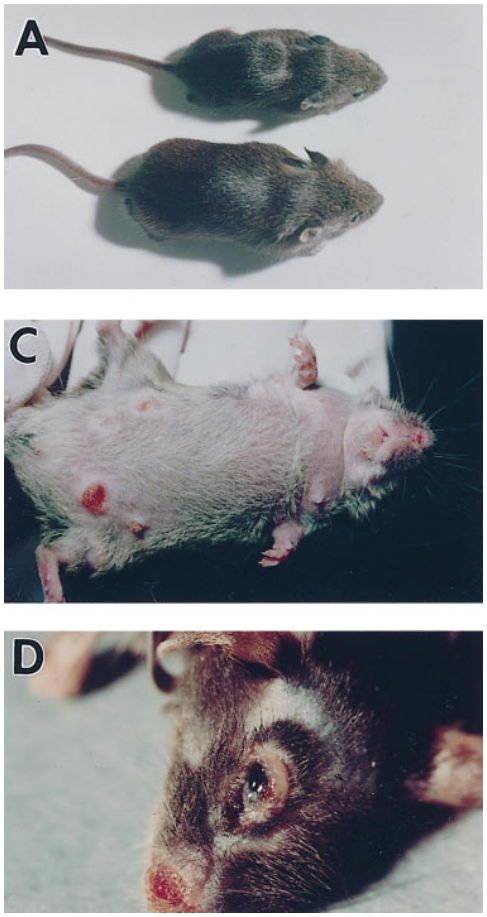

Figure 3. DSG3 −/− mice are runts and have skin erosions and eye lesions. (*A*) DSG3 −/− mice are runts. Upper mouse is DSG3 −/−; lower mouse is a +/+ littermate. (*B*) Weight graph shows that −/− mice (*open circles*), compared with +/+ and +/− littermates (*filled circles*), are born with equal weight but by about day 8–10 are lagging in weight gain. Weight loss is seen about day 20, approximately the time of weaning and start of solid food. (*C*) Nipple erosions in a DSG3 −/− nursing mother. (*D*) Snout erosion and conjunctivitis in a DSG3 −/− mouse.

DSG3 −/− Mice Show Loss of Keratinocyte Cell Adhesion Resulting in a Phenotype That Resembles That of Patients with PV

Around 15–20 d after birth, −/− animals differed in size from +/− and +/+ animals. The −/− mutants were much smaller than their littermates (Fig. 3 *A*). Autopsies revealed a dramatic reduction in body fat in the −/− animals that resembles what is seen in starvation.

Runting of the pups consistently sorted with the targeted mutation and was never observed in animals that were wild type or heterozygous for the mutant allele. A closer analysis revealed that at birth all pups showed similar weights, but, at 8–10 d after birth, −/− animals showed reduced bodyweight (Fig. 3 *B*). In the following days, the mutants grew at a much slower rate than +/− and +/+ mice. Between days 18 and 25, the growth of −/− animals slowed down even more with most mutants losing weight and a few dying (Fig. 3 *B*). However, >80% of mutants survived and again started to gain weight, but they were still clearly smaller than their littermates. No significant weight difference between +/− and +/+ mice was observed.

Since the most characteristic lesions in pemphigus vulgaris patients are painful oral erosions that may interfere with eating, we speculated that the DSG3 −/− animals might have similar lesions preventing them from feeding sufficiently that would, in turn, result in runting. Indeed, histological examination of the oral mucosa in DSG3 −/− mice showed a full spectrum of the types of lesions typical of PV. The most common lesion was an inflammatory erosion, sometimes seen with reepithelialization (Fig. 4 *A*). This is typical of a late PV blister after the superficial epidermis is lost and the resulting irritation and/or colonization of the erosion results in acute inflammation and loss of the basal cells (Fig. 4 *B*). Further examination showed intermediate lesions with the superficial epidermis lost, leaving the basal cells still attached to the basement membrane, but slightly detached from each other (Fig. 4 *C*). This appearance has been called the "row of tombstones" in patients with PV (Fig. 4 *D*). Finally, we could also detect the earliest lesion of PV in the DSG3 −/− mice, namely a suprabasilar split in the epithelium, with minimal inflammation (Fig. 4 *E*). Oropharyngeal biopsies of essentially all DSG3 −/− mice, examined at ages 3 d–5 mo, showed these changes, but DSG3 +/− and +/+ mice never showed them. We speculate from this data that suckling resulted in the trauma necessary to cause these lesions initially, with the beginning of solid food at 16–20 d exacerbating them. The resulting lesions presumably decreased food intake enough to result in the runting of these mice.

Interestingly, the epidermis of these mice did not show extensive spontaneous lesions. However, when a female DSG3 −/− mouse delivered pups, their suckling caused erosions around the nipples (Fig. 3 *C*) and some mice

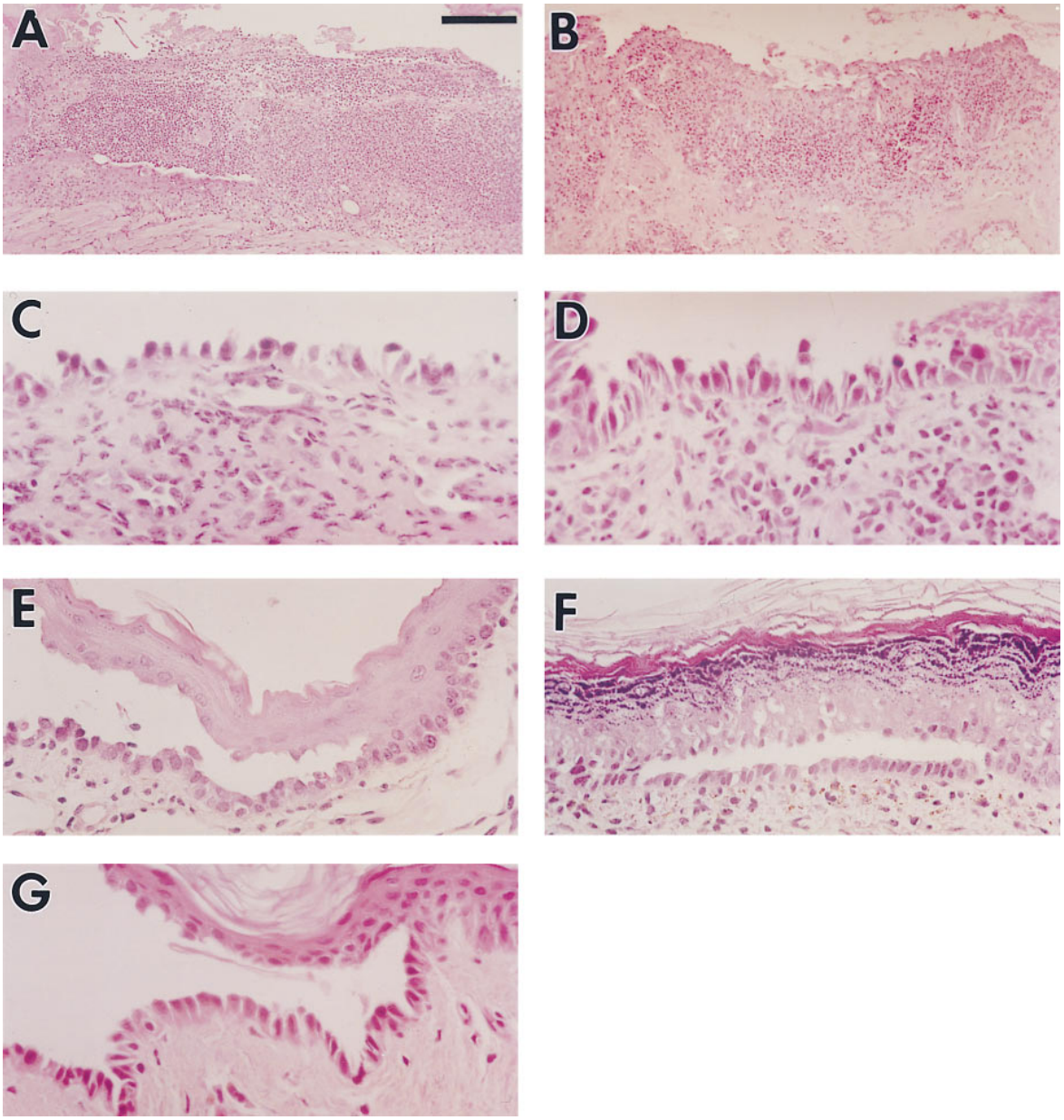

Figure 4. Histology of oral mucous membranes and skin in DSG3 −/− mice and human PV patients. (*A*) DSG3 −/−: inflammatory oral erosion of the tongue. (*B*) Human PV: inflammatory oral erosion. (*C*) DSG3 −/−: oral lesion shows basal cells are separated from each other and the suprabasilar epithelium is lost. This is a characteristic histology called a "row of tombstones." (*D*) Human PV: oral lesion shows a "row of tombstones." (*E*) DSG3 −/−: early oral lesion shows suprabasilar acantholysis with intact suprabasilar epithelium separated from basal cells. (*F*) DSG3 −/−: early skin lesion on dorsum of foot near where skin was traumatized by cutting. (*G*) Human PV: skin lesion shows typical suprabasilar acantholysis. Bar: (*A* and *B*) 160 μm; (*C–G*) 40 μm.

showed crusting on the skin around the eyes and snout (Fig. 3 *D*), areas that are normally traumatized by scratching. Histology of traumatized skin also showed typical suprabasilar blisters (Fig. 4 *F*), similar to the histology of skin lesions in pemphigus vulgaris patients (Fig. 4 *G*). Some DSG3 −/− mice also showed suppurative conjunctivitis (Fig. 3 *D*) with suprabasilar blisters of eyelids and mucocutaneous conjunctiva, similar to what has been reported in patients (Hodak et al., 1990).

Among the other stratified epithelia examined, only the vaginal epithelium of a DSG3 −/− mouse showed suprabasilar blistering. Histology of the esophagus, the cardiac portion of the stomach, and the thymus (for Dsg3 expression in thymus see Schäfer et al., 1994) revealed no abnormalities.

EM of nonlesional epidermis and lingual mucosa in DSG3 −/− mice showed normal differentiation. Desmosomes were present, and individual desmosomes appeared indistinguishable from those of unaffected littermates: both had well-defined membrane lipid bilayers, intracellular dense plaques anchored to aggregated intermediate filaments, and extracellular domains with typical central,

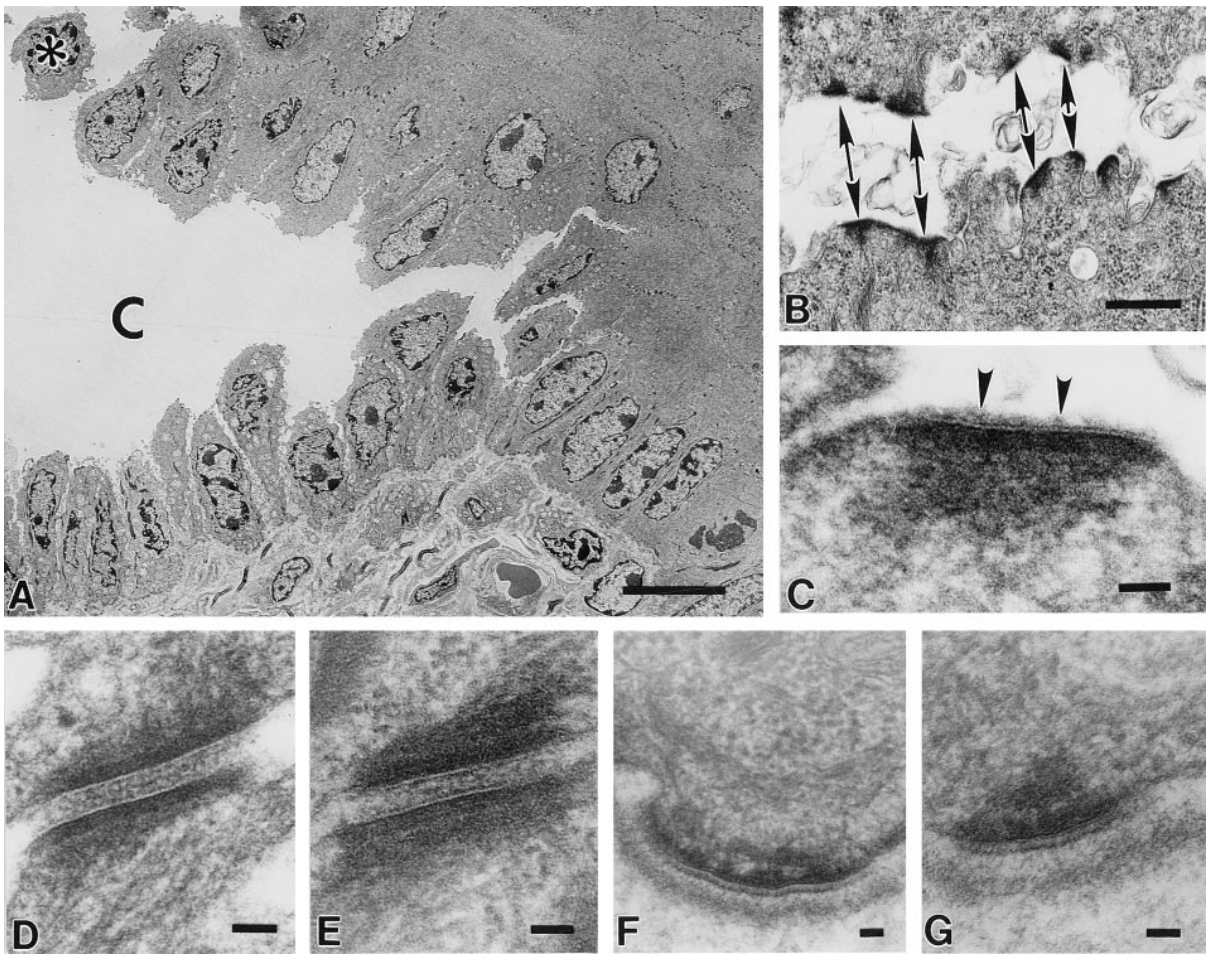

Figure 5. Ultrastructure of lesional posterior lingual epithelium in DSG3 −/− mice. (*A*) An edge of a blister cavity, denoted by "C" in a DSG3 −/− mouse. The base is formed by a single layer of basal keratinocytes with a characteristic "tombstone" cytoarchitecture. The roof consists of intact suprabasal epithelium with occasional associated acantholytic keratinocytes (*). (*B*) Blister in a DSG3 −/− mouse shows separation of desmosomes which form half-desmosomes (*double arrows*) with tonofilaments still attached. (*C*) Higher magnification of a half-desmosome shows an intact intracytoplasmic dense plaque and its associated tonofilaments. There is residual flocculent material (*arrowheads*) along the cell membrane. (*D*) Desmosome in DSG3 +/+ littermate. (*E*) Desmosome in DSG3 −/− mouse has normal appearance. (*F*) Hemidesmosome in DSG3 +/+ littermate. (*G*) Hemidesmosome in DSG3 −/− mouse shows normal appearance. Bars: (*A*) 10 μm; (*B*) 0.5 μm; (*C–G*) 50 nm.

electron-dense disks formed by flocculent material (Fig. 5, *D* and *E*). The extracellular domains were consistently 20–25 nm thick in both control and affected animals. Our general impression was that the number of desmosomes in DSG3 −/− mice may have been diminished focally along the lateral and apical surfaces of basal cells, but, as a result of the focal nature of this finding, we could not quantitate it convincingly. EM of lesions in DSG3 −/− mice showed cellular detachment primarily at the apical and lateral surfaces of the basal cells (Fig. 5, *A* and *B*). Accordingly, the acantholytic cleft was formed as a result of separation of basal cells from suprabasal cells and from each other at the cell membranes. Hemidesmosomes were structurally normal (Fig. 5, *F* and *G*). Separated acantholytic cells retained "half" desmosomes, containing the intracytoplasmic dense plaque with attached intermediate filaments, along the plasma membrane that abutted the cleavage plane (Fig. 5 *C*). These half desmosomes contained a finely flocculent material (i.e., desmoglea) on their extracellular surface. These residual half desmosomes were particularly prominent along the apical surfaces of basal cells and tended to aggregate and coalesce. Individual intact desmosomes directly adjacent to acantholytic areas appeared normal.

An additional, and unexpected, phenotype developed at around the time of weaning (3–4 wk after birth) in DSG3 −/− mice. They started to lose their hair and developed completely bald areas, first on the forehead, and then proceeding onto the entire back (Fig. 6 *A*). This phenomenon was observed whether the mutants were housed in groups or alone. The ventral coat at this age seemed thin but basically intact. New hair regrowth started from the head to the back. These cycles of hair loss and regrowth occurred repeatedly, but after two to three cycles they lost the head to tail synchronization and occurred as bald patches with regrowth, involving both the ventral and dorsal coats. As hair loss is not a major finding in PV patients, this phenotype either is specific for a genetic loss of Dsg3 or is peculiar to mice as opposed to humans.

There were no phenotypic abnormalities of any kind observed in DSG3 +/− mice.

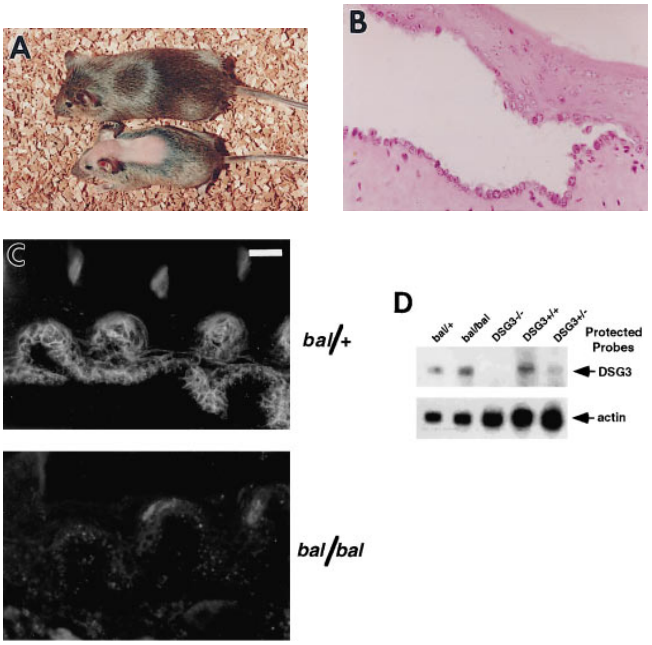

Figure 6. Analysis of balding mice compared with DSG3 −/− mice. (*A*) Balding phenotype of a 1-mo-old DSG3 −/− mouse compared with a normal littermate (above). (*B*) Histology of an oral mucosal blister in a *bal*/*bal* mouse shows suprabasilar acantholysis. (*C*) Immunofluorescence of *bal*/*bal* tongue shows no Dsg3 compared with control littermate. (*D*) RNase protection assay of tongue lysates demonstrates that *bal*/*bal* mice synthesize DSG3 mRNA, as compared with DSG3 −/− mice that do not. Note that DSG3 +/− mice demonstrate about half of the mRNA of wild-type mice.

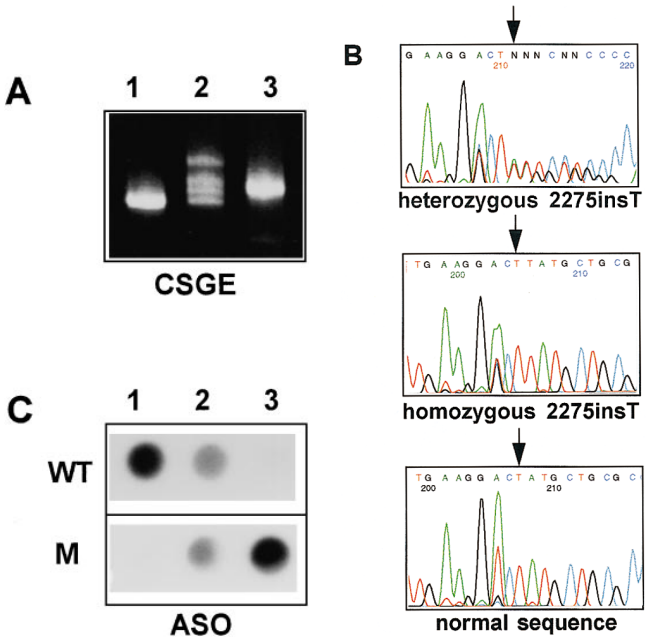

Figure 7. Analysis of the DSG3 mutation in balding mice. (*A*) Heteroduplex analysis of a 400-bp segment of PCR-amplified mouse DSG3, containing exon 14 and flanking intronic sequences, revealed heteroduplex bands in case of a heterozygous *bal*/+ mouse (lane *2*), while control mouse (lane *1*) and a homozygous *bal*/*bal* (lane *3*) showed a homoduplex band only. (*B*) Direct nucleotide sequencing of DNA shown on lane *2* in *A* revealed a heterozygous 1-bp insertion, 2275insT, which resulted in frame-shift (*upper panel*), in comparison with normal sequence in DNA obtained from a control mouse shown on lane *1* in *A* (*lower panel*). Sequencing of DNA on lane *3* revealed that *bal*/*bal* mouse was homozygous for the 2275insT mutation (*middle panel*). (*C*) Allele-specific oligonucleotide hybridization (*ASO*) was used to verify the presence of the mutation in balding mice. Specifically, PCR-amplified DNA from the control mouse hybridized with the wild-type oligomer (*WT*) only (lane *1*), while homozygous *bal*/*bal* mouse hybridized with the mutant (*M*) probe only (lane *3*). DNA from *bal*/+ mouse hybridized with both the WT and M probes, indicating that these mice were heterozygous for the mutation (lane *2*).

Balding (bal) Mice Have the Same Phenotype as DSG3 −/− Mice and Have a Null Mutation in the DSG3 Gene

The phenotype of runting and hair loss around the time of weaning seen in the DSG3 −/− mutants has been described in mice with a spontaneous mutation termed *bal* (Sundberg, 1994). This recessive mutation has recently been mapped to a position close to the DSG3 locus on mouse chromosome 18 (Davisson et al., 1994). We therefore speculated that *bal* might be a DSG3 null mutation.

Histological analysis revealed the presence of suprabasilar blisters on the tongue of *bal*/*bal* mice, indistinguishable from those found in our DSG3 −/− mice (Fig. 6 *B*). These lesions were never found in *bal*/+ or +/+ littermates.

We then determined whether the balding mutation and our targeted mutation were coallelic. A mouse heterozygous for the targeted mutation (DSG3 +/−) was bred to a mouse heterozygous for the *bal* mutation (*bal*/+). Two of the seven pups obtained from these crosses were runts. Furthermore, histological analysis demonstrated the presence of multiple lesions in the oropharynx of the runts (but not the normal size littermates) with the typical PV-like morphology (data not shown). By Southern blot analysis, we showed that one runt possessed a targeted DSG3 allele, and mutation analysis (see below) demonstrated the presence of the heterozygous balding mutation as well (data not shown). Additionally, at the time of weaning, these runts lost their hair in a pattern identical to that described above for the mice with the targeted DSG3 mutation. We conclude that the runt had inherited the targeted allele from one parent and the *bal* mutation from the other, and developed the same phenotype as DSG3 −/− and *bal*/*bal* mice. These data demonstrate that the targeted mutation and the balding mutation are coallelic.

Further analysis of the balding mice by immunofluorescence microscopy on tongue epithelium from mice heterozygous (*bal*/+) and homozygous (*bal*/*bal*) for the balding mutation was done using antibodies against extracellular and intracellular epitopes of Dsg3. Whereas *bal*/+ epithelium clearly stained with these antibodies, no staining was observed in the *bal*/*bal* epithelium (Fig. 6 *C*). Control antibodies against desmoglein 1 and 2, desmoplakin and plakoglobin stained both *bal*/+ and *bal*/*bal* epithelia equally well (data not shown). However, using an RNase protection assay, we were able to detect a transcript derived from the DSG3 locus (Fig. 6 *D*). Given the fact that we did not detect Dsg3 by immunofluorescence analysis, we hypothe-

sized that a mutation within the *DSG3* gene of the *bal*/*bal* mutants leads to a transcript that is either not translated or that directs the synthesis of a truncated polypeptide that is rapidly degraded. We therefore screened the *DSG3* gene for putative mutations by heteroduplex analysis. Band shifting of PCR products derived from exon 14 of the obligate heterozygous *bal*/+ mouse suggested the presence of a mutation in the *DSG3* gene (Fig. 7 *A*). Sequence analysis of this aberrant PCR fragment identified heterozygous insertion of a thymidine residue at a position that would correspond to nucleotide 2,418 in the human cDNA (Amagai et al., 1991), as determined by the nucleotide and aa homology in this region with the mouse sequence (Fig. 7 *B*). This insertion causes a frame-shift resulting in a premature stop codon 78 bp downstream from the site of insertion. The *bal*/*bal* mouse was homozygous for the insertion (Fig. 7 *B*). The presence of the insertion mutation was verified by allele-specific oligonucleotide hybridization (Fig. 7 *C*). By homology to the reported human sequence, the mutated transcript would encode a polypeptide that lacks most of the intracellular domain of Dsg3 (after aa 778 [Amagai et al., 1991]), in particular the amino acid sequence to which plakoglobin binds (Mathur et al., 1994; Troyanovsky et al., 1994; Roh and Stanley, 1995; Chitaev et al., 1996; Kowalczyk et al., 1996). The fact that the Dsg3 antibodies used in this study (e.g., those that bind extracellular epitopes and an intracellular epitope encoded upstream of the frame-shift mutation) did not stain *bal*/*bal* epithelium strongly suggests that a truncated Dsg3 polypeptide, if synthesized in these mice, is not inserted into the plasma membrane and/or is rapidly degraded.

Both the absence of Dsg3 immunostaining and the presence of suprabasilar blisters indicate that the balding mouse represents a functional DSG3 null mutation.

Histology of the bald area in DSG3 −/− mice shows slightly cystic telogen hair follicles that lack a hair shaft (Fig. 8). Further detailed analysis will be needed to determine the exact cause of this hair loss.

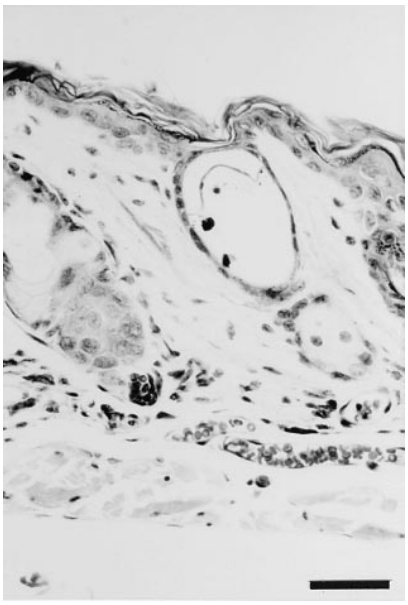

Figure 8. Histology of bald back skin from a 24-d-old DSG3 −/− mouse. Note dilated telogen hair follicle containing a clump of pigment but no hair shaft. Bar, 35 μm.

Discussion

It has proven difficult, using in vitro methods, to demonstrate whether desmogleins mediate cell adhesion because they normally are organized in the desmosome with multiple other proteins that may affect their function. A direct way to analyze their function in vivo is to determine what happens to cell adhesion if one desmoglein is eliminated. We therefore genetically engineered a mouse with a targeted disruption of DSG3.

The phenotype of this mouse resembled in many, but not all, ways that of patients with PV who have autoantibodies directed against DSG3. Painful oral mucous membrane erosions resulting from suprabasilar acantholysis are the most characteristic lesions of PV (Lever, 1965). Patients often present with oral mucous membrane lesions, and these may persist, without skin lesions, for months. Some patients only have oral lesions. Patients may lose weight and become dehydrated because these painful lesions often interfere with normal food and fluid intake. Similarly, the major lesions in DSG3 −/− mice were oral mucous membrane erosions. As in PV patients, early lesions showed suprabasilar acantholysis with later lesions showing inflammatory erosions. We presume that these lesions interfered with oral intake, as these mice, which were born with normal weights, became runts once they relied on oral intake for food. We noticed individual variations in the severity of the mutant phenotype; i.e., a few animals died whereas most reached adulthood. These variations were not unexpected and might be, at least in part, due to the presence of "modifier genes" in this outbred line. Finally, electron microscopic analysis of a blister in DSG3 −/− mice reveals very similar findings to those of patients' lesions. In both, separating desmosomes are seen, with acantholytic cells showing single attachment plaques to which tonofilaments insert (Lever, 1979).

Unlike some patients, these mice did not develop extensive spontaneous skin lesions, but did develop some crusted lesions around the eyes, on the snout, and on the nipples of a nursing mother, resulting presumably from trauma. The skin and mucocutaneous junction of the eyelids also showed histologically typical pemphigus lesions as did some biopsies near the edges where skin was traumatized in cutting. An analogous phenomenon, called the Nikolski sign, occurs in patients with active PV in whom rubbing on normal skin may cause erosions with resultant crusting (Lever, 1965). The findings of conjunctivitis and PV-like lesions in the eyes of DSG3 −/− mice have also been reported in patients (Hodak et al., 1990).

The fact that skin of mice is very different from that of humans, with many more hair follicles, may account for the finding that most skin areas in mice do not develop extensive erosions. Furthermore, mice may not develop skin erosions as extensive as those sometimes seen in humans because, as discussed in the Introduction, autoantibody binding to human skin might stimulate release of proteases that could amplify blister formation. In addition, the hair phenotype of these mice may be a reflection of the

difference in hair in rodents and humans, as humans with PV usually do not develop a balding phenotype. Preliminary analysis of the hair phenotype in these mice shows a normal first hair cycle but loss of hair after this cycle. In bald areas, histology of the skin reveals dilated telogen follicles lacking a hair shaft. Previous analysis of balding mice has shown necrosis immediately above the hair matrix leading to some scattered generalized follicular necrosis (Sundberg, 1994). Additional analysis will be required to better define the pathophysiology of hair loss in these DSG3 −/− and balding mice.

Moreover, considering the major difference in mouse and human stratified squamous epithelia and adnexal structures, it is remarkable how similar the phenotype of DSG3 −/− mice is to PV patients.

The phenotype of Dsg3 −/− mice is quite different from that of a recently described transgenic mouse that expresses an amino-terminal deleted Dsg3 under the control of the K14 promoter (Allen et al., 1996). The transgene used consisted of the cytoplasmic and transmembrane domain as well as part of the extracellular domain of Dsg3 and was expressed mainly in the lower layers of the epidermis. The transgenic mice, thought to express a dominant negative effect of the truncated Dsg3, showed swelling of paws and digits, focal flakiness of the skin, and necrotic changes on the tips of the tails that ultimately resulted in tail degeneration. Furthermore, histological analysis revealed epidermal thickening and widening of the intercellular space between keratinocytes but did not show loss of cell–cell adhesion (i.e., acantholysis). At the ultrastructural level, a reduction in the number of desmosomes and the occurrence of aberrant desmosomes were reported. Although these mice were noted to have a wet and matted hair coat (probably because of excess grooming), they did not show an obvious loss of hair. Our DSG3 −/− mice clearly had a different phenotype and distinct histologic and ultrastructural abnormalities. DSG3 −/− mice did not show any tail abnormality and did not have flaky skin, but they developed crusted erosions in areas of trauma. They also had a striking balding phenotype. Histologically these mice showed obvious acantholysis. Finally, ultrastructurally, the DSG3 −/− mice showed normally appearing desmosomes in intact skin and "half"-desmosomes where cells were acantholytic. We conclude from these differences between the transgenic and DSG3 −/− mice that the truncated Dsg3 did not act in a dominant negative fashion to totally inactivate DSG3 function.

The phenotype of DSG3 knockout mice underscores the importance of Dsg3 for cell adhesion and mechanical stability in the deepest layers of stratified epithelia. The other transmembrane adhesion molecules present, such as Dsg2, desmocollins, E-cadherin, and P-cadherin, apparently cannot compensate for the loss of Dsg3. In addition, Dsg3 seems to be particularly important for adhesion in the oral mucous membrane, where lesions always occurred in DSG3 −/− mice, and less so in other stratified squamous epithelia such as esophagus where lesions were never seen. The importance of Dsg3 in skin seems intermediate because lesions were mainly seen secondary to trauma. These studies, then, show that specific desmogleins may have tissue- and differentiation-specific adhesion functions.

Finally, the phenotype of the Dsg3 knockout mice not only demonstrates the importance of Dsg3 for cell adhesion in the deep stratified squamous epithelia, but also is consistent with the idea that, at least in part, PV autoantibodies cause loss of cell adhesion by directly interfering with the adhesive function of Dsg3.

We thank Dr. Chin Howe for valuable discussions and advice regarding knockout technology; Dr. Victor Tybulewicz for providing the targeting vector; Daniela Simon who did karyotyping; Dr. Jean Richa, from the University of Pennsylvania Transgenic Facility, who performed the ES cell injections; Qi Tian, Drs. Stephan Schäfer, and Werner Franke for providing Dsg2 cDNA and antibodies; Dr. Margaret Wheelock for plakoglobin antibodies; Dr. Kehua Li for assistance in cloning the mouse *DSG3* gene; and Dr. Sarolta Karpati for helping with anti-Dsg3 antibody preparation.

This work was supported by National Institutes of Health grants 1RO1AR43776, PO1AR38923, and CA20408. P. Koch was supported by The Thyssen Foundation and a research fellowship from the Dermatology Foundation.

Received for publication 3 February 1997 and in revised form 20 March 1997.

References

Akiyama, M., T. Hashimoto, M. Sugiura, and T. Nishikawa. 1991. Ultrastructural localization of pemphigus vulgaris and pemphigus foliaceus antigens in cultured human squamous carcinoma cells. *Br. J. Dermatol.* 125:233–237.

Allen, E., Q.C. Yu, and E. Fuchs. 1996. Mice expressing a mutant desmosomal cadherin exhibit abnormalities in desmosomes, proliferation, and epidermal differentiation. *J. Cell Biol.* 133:1367–1382.

Amagai, M., V. Klaus-Kovtun, and J.R. Stanley. 1991. Autoantibodies against a novel epithelial cadherin in pemphigus vulgaris, a disease of cell adhesion. *Cell.* 67:869–877.

Amagai, M., S. Karpati, R. Prussick, V. Klaus-Kovtun, and J.R. Stanley. 1992. Autoantibodies against the amino-terminal cadherin-like binding domain of pemphigus vulgaris antigen are pathogenic. *J. Clin. Invest.* 90:919–926.

Amagai, M., T. Hashimoto, N. Shimizu, and T. Nishikawa. 1994*a.* Absorption of pathogenic autoantibodies by the extracellular domain of pemphigus vulgaris antigen (Dsg3) produced by baculovirus. *J. Clin. Invest.* 94:59–67.

Amagai, M., S. Karpati, V. Klaus-Kovtun, M.C. Udey, and J.R. Stanley. 1994*b.* The extracellular domain of pemphigus vulgaris antigen (desmoglein 3) mediates weak homophilic adhesion. *J. Invest. Dermatol.* 102:402–408.

Amagai, M., P.J. Koch, T. Nishikawa, and J.R. Stanley. 1996. Pemphigus vulgaris antigen (Desmoglein 3) is localized in the lower epidermis, the site of blister formation in patients. *J. Invest. Dermatol.* 106:351–355.

Arnemann, J., K.H. Sullivan, A.I. Magee, I.A. King, and R.S. Buxton. 1993. Stratification-related expression of isoforms of the desmosomal cadherins in human epidermis. *J. Cell Sci.* 104:741–750.

Blaschuk, O.W., R. Sullivan, S. David, and Y. Pouliot. 1990. Identification of a cadherin cell adhesion recognition sequence. *Dev. Biol.* 139:227–229.

Buxton, R.S., P. Cowin, W.W. Franke, D.R. Garrod, K.J. Green, I.A. King, P.J. Koch, A.I. Magee, D.A. Rees, J.R. Stanley, and M.S. Steinberg. 1993. Nomenclature of the desmosomal cadherins. *J. Cell Biol.* 121:481–483.

Chidgey, M.A., J.P. Clarke, and D.R. Garrod. 1996. Expression of full-length desmosomol glycoproteins (desmocollins) is not sufficient to confer strong adhesion on transfected L929 cells. *J. Invest. Dermatol.* 106:689–695.

Chitaev, N.A., R.E. Leube, R.B. Troyanovsky, L.G. Eshkind, W.W. Franke, and S.M. Troyanovsky. 1996. The binding of plakoglobin to desmosomal cadherins: patterns of binding sites and topogenic potential. *J. Cell Biol.* 133: 359–369.

Collins, J.E., P.K. Legan, T.P. Kenny, J. MacGarvie, J.L. Holton, and D.R. Garrod. 1991. Cloning and sequence analysis of desmosomal glycoproteins 2 and 3 (desmocollins): cadherin-like desmosomal adhesion molecules with heterogeneous cytoplasmic domains. *J. Cell. Biol.* 113:381–391.

Davisson, M.T., S.A. Cook, K.R. Johnson, and E.M. Eicher. 1994. Balding: a new mutation on mouse chromosome 18 causing hair loss and immunological defects. *J. Hered.* 85:134–136.

Farb, R.M., R. Dykes, and G.S. Lazarus. 1978. Anti-epidermal-cell-surface pemphigus antibody detaches viable epidermal cells from culture plates by activation of proteinase. *Proc. Natl. Acad. Sci. USA.* 75:459–463.

Ganguly, A., M.J. Rock, and D.J. Prockop. 1993. Conformation-sensitive gel electrophoresis for rapid detection of single base differences in double-stranded PCR products and DNA fragments: evidence for solvent-induced bends in DNA heteroduplexes. *Proc. Natl. Acad. Sci. USA.* 90:10325–10329.

Goodwin, L., J.E. Hill, K. Raynor, L. Raszi, M. Manabe, and P. Cowin. 1990. Desmoglein shows extensive homology to the cadherin family of cell adhesion molecules. *Biochem. Biophys. Res. Commun.* 173:1224–1230.

Hashimoto, K., K.M. Shafran, P.S. Webber, G.S. Lazarus, and K.H. Singer.

1983. Anti-cell surface pemphigus autoantibody stimulates plasminogen activator activity of human epidermal cells. *J. Exp. Med.* 157:259–272.

Hashimoto, K., T.C. Wun, J. Baird, G.S. Lazarus, and P.J. Jensen. 1989. Characterization of keratinocyte plasminogen activator inhibitors and demonstration of the prevention of pemphigus IgG-induced acantholysis by a purified plasminogen activator inhibitor. *J. Invest. Dermatol.* 92:310–314.

Hodak, E., I. Kremer, M. David, B. Hazaz, A. Rothem, P. Feuerman, and M. Sandbank. 1990. Conjunctival involvement in pemphigus vulgaris: a clinical, histopathological and immunofluorescence study. *Br. J. Dermatol.* 123:615–620.

Hogan, B., R. Beddington, F. Costantini, and E. Lacy. 1994. Manipulating the Mouse Embryo. Cold Spring Harbor Laboratory, Cold Spring Harbor, NY. 497 pp.

Horie, K., S. Nishiguchi, S. Maeda, and K. Shimada. 1994. Structures of replacement vectors for efficient gene targeting. *J. Biochem. (Tokyo).* 115:477–485.

Ishikawa, H., S.A. Silos, K. Tamai, N.G. Copeland, D.J. Gilbert, N.A. Jenkins, and J. Uitto. 1994. cDNA cloning and chromosomal assignment of the mouse gene for desmoglein 3 (Dsg3), the pemphigus vulgaris antigen. *Mamm. Genome.* 5:803–804.

Karpati, S., M. Amagai, R. Prussick, K. Cehrs, and J.R. Stanley. 1993. Pemphigus vulgaris antigen, a desmoglein type of cadherin, is localized within keratinocyte desmosomes. *J. Cell Biol.* 122:409–415.

King, I.A., J. Arnemann, N.K. Spurr, and R.S. Buxton. 1993. Cloning of the cDNA (DSC1) coding for human type 1 desmocollin and its assignment to chromosome 18. *Genomics.* 18:185–194.

Koch, P.J., and W.W. Franke. 1994. Desmosomal cadherins: another growing multigene family of adhesion molecules. *Curr. Opin. Cell Biol.* 6:682–687.

Koch, P.J., M.J. Walsh, M. Schmelz, M.D. Goldschmidt, R. Zimbelmann, and W.W. Franke. 1990. Identification of desmoglein, a constitutive desmosomal glycoprotein, as a member of the cadherin family of cell adhesion molecules. *Eur. J. Cell Biol.* 53:1–12.

Koch, P.J., M.D. Goldschmidt, M.J. Walsh, R. Zimbelmann, and W.W. Franke. 1991*a.* Complete amino acid sequence of the epidermal desmoglein precursor polypeptide and identification of a second type of desmoglein gene. *Eur. J. Cell Biol.* 55:200–208.

Koch, P.J., M.D. Goldschmidt, M.J. Walsh, R. Zimbelmann, M. Schmelz, and W.W. Franke. 1991*b.* Amino acid sequence of bovine muzzle epithelial desmocollin derived from cloned cDNA: a novel subtype of desmosomal cadherins. *Differentiation.* 47:29–36.

Koch, P.J., M.D. Goldschmidt, R. Zimbelmann, R. Troyanovsky, and W.W. Franke. 1992. Complexity and expression patterns of the desmosomal cadherins. *Proc. Natl. Acad. Sci. USA.* 89:353–357.

Kowalczyk, A.P., J.E. Borgwardt, and K.J. Green. 1996. Analysis of desmosomal cadherin-adhesive function and stoichiometry of desmosomal cadherin-plakoglobin complexes. *J. Invest. Dermatol.* 107:293–300.

Lavker, R.M., G. Dong, P. Zheng, and G.F. Murphy. 1991. Hairless micropig skin. A novel model for studies of cutaneous biology. *Am. J. Pathol.* 138: 687–697.

Lever, W.F. 1965. Pemphigus and Pemphigoid. Charles C. Thomas, Springfield, IL. 266 pp.

Lever, W.F. 1979. Pemphigus and pemphigoid. *J. Am. Acad. Dermatol.* 1:2–31.

Mansour, S.L., K.R. Thomas, and M.R. Capecchi. 1988. Disruption of the proto-oncogene int-2 in mouse embryo-derived stem cells: a general strategy for targeting mutations to non-selectable genes. *Nature (Lond.).* 336:348–352.

Mathur, M., L. Goodwin, and P. Cowin. 1994. Interactions of the cytoplasmic domain of the desmosomal cadherin dsg1 with plakoglobin. *J. Biol. Chem.* 269:14075–14080.

Mechanic, S., K. Raynor, J.E. Hill, and P. Cowin. 1991. Desmocollins form a distinct subset of the cadherin family of cell adhesion molecules. *Proc. Natl. Acad. Sci. USA.* 88:4476–4480.

Memar, O.M., S. Rajaraman, R. Thotakura, S.K. Tyring, J.L. Fan, G.S. Seetharamaiah, A. Lopez, R.E. Jordon, and B.S. Prabhakar. 1996. Recombinant desmoglein 3 has the necessary epitopes to adsorb and induce blister-causing antibodies. *J. Invest. Dermatol.* 106:261–268.

Morioka, S., G.S. Lazarus, and P.J. Jensen. 1987. Involvement of urokinase-type plasminogen activator in acantholysis induced by pemphigus IgG. *J. Invest. Dermatol.* 89:474–477.

Nagafuchi, A., Y. Shirayoshi, K. Okazaki, K. Yasuda, and M. Takeichi. 1987. Transformation of cell adhesion properties by exogenously introduced E-cadherin cDNA. *Nature (Lond.).* 329:341–343.

Naito, K., S. Morioka, S. Nakajima, and H. Ogawa. 1989. Proteinase inhibitors block formation of pemphigus acantholysis in experimental models of neonatal mice and skin explants: effects of synthetic and plasma proteinase inhibitors on pemphigus acantholysis. *J. Invest. Dermatol.* 93:173–177.

Nilles, L.A., D.A.D. Parry, E.E. Powers, B.D. Angst, R.M. Wagner, and K.J. Green. 1991. Structural analysis and expression of human desmoglein: a cadherin-like component of the desmosome. *J. Cell Sci.* 99:809–821.

North, A.J., M.A. Chidgey, J.P. Clarke, W.G. Bardsley, and D.R. Garrod. 1996. Distinct desmocollin isoforms occur in the same desmosomes and show reciprocally graded distributions in bovine nasal epidermis. *Proc. Natl. Acad. Sci. USA.* 93:7701–7705.

Nose, A., K. Tsuji, and M. Takeichi. 1990. Localization of specificity determining sites in cadherin cell adhesion molecules. *Cell.* 61:147–155.

Nuber, U.A., S. Schäfer, A. Schmidt, P.J. Koch, and W.W. Franke. 1995. The widespread human desmocollin Dsc2 and tissue-specific patterns of synthesis of various desmocollin subtypes. *Eur. J. Cell Biol.* 66:69–74.

Nuber, U.A., S. Schäfer, S. Stehr, H.R. Rackwitz, and W.W. Franke. 1996. Patterns of desmocollin synthesis in human epithelia: immunolocalization of desmocollins 1 and 3 in special epithelia and in cultured cells. *Eur. J. Cell Biol.* 71:1–13.

Parker, A.E., G.N. Wheeler, J. Arnemann, S.C. Pidsley, P. Ataliotis, C.L. Thomas, D.A. Rees, A.I. Magee, and R.S. Buxton. 1991. Desmosomal glycoproteins II and III. Cadherin-like junctional molecules generated by alternative splicing. *J. Biol. Chem.* 266:10438–10445.

Ramirez-Solis, R., J. Rivera-Perez, J.D. Wallace, M. Wims, H. Zheng, and A. Bradley. 1992. Genomic DNA microextraction: a method to screen numerous samples. *Anal. Biochem.* 201:331–335.

Ramirez-Solis, R., A.C. Davis, and A. Bradley. 1993. Gene targeting in embryonic stem cells. *Methods Enzymol.* 225:855–879.

Roh, J.Y., and J.R. Stanley. 1995. Plakoglobin binding by human Dsg3 (pemphigus vulgaris antigen) in keratinocytes requires the cadherin-like intracytoplasmic segment. *J. Invest. Dermatol.* 104:720–724.

Sambrook, J., E.F. Fritsch, and T. Maniatis. 1989. Molecular Cloning: A Laboratory Manual. Cold Spring Harbor Laboratory, Cold Spring Harbor, NY. 545 pp.

Schäfer, S., P.J. Koch, and W.W. Franke. 1994. Identification of the ubiquitous human desmoglein, Dsg2, and the expression catalogue of a subfamily of desmosomal cadherins. *Exp. Cell Res.* 211:391–399.

Schäfer, S., S. Stumpp, and W.W. Franke. 1996. Immunological identification and characterization of the desmosomal cadherin Dsg2 in coupled and uncoupled epithelial cells and in human tissues. *Differentiation.* 60:99–108.

Schiltz, J.R., B. Michel, and R. Papay. 1978. Pemphigus antibody interaction with human epidermal cells in culture. *J. Clin. Invest.* 62:778–788.

Schiltz, J.R., B. Michel, and R. Papay. 1979. Appearance of "pemphigus acantholysis factor" in human skin cultured with pemphigus antibody. *J. Invest. Dermatol.* 73:575–581.

Schmidt, A., H.W. Heid, S. Schäfer, U.A. Nuber, R. Zimbelmann, and W.W. Franke. 1994. Desmosomes and cytoskeletal architecture in epithelial differentiation: cell type-specific plaque components and intermediate filament anchorage. *Eur. J. Cell Biol.* 65:229–245.

Schwarz, M.A., K. Owaribe, J. Kartenbeck, and W.W. Franke. 1990. Desmosomes and hemidesmosomes: constitutive molecular components. *Annu. Rev. Cell Biol.* 6:461–491.

Shimizu, H., T. Masunaga, A. Ishiko, A. Kikuchi, T. Hashimoto, and T. Nishikawa. 1995. Pemphigus vulgaris and pemphigus foliaceus sera show an inversely graded binding pattern to extracellular regions of desmosomes in different layers of human epidermis. *J. Invest. Dermatol.* 105:153–159.

Stanley, J.R. 1990. Pemphigus: skin failure mediated by autoantibodies. *JAMA (J. Am. Med. Assoc.).* 264:1714–1717.

Stanley, J.R. 1993*a.* Pemphigus. *In* Dermatology in General Medicine. T.B. Fitzpatrick, A.Z. Eisen, K. Wolff, I.M. Freedberg, and K.F. Austen, editor. McGraw-Hill, New York. 606–615.

Stanley, J.R. 1993*b.* Cell adhesion molecules as targets of autoantibodies in pemphigus and pemphigoid, bullous diseases due to defective epidermal cell adhesion. *Adv. Immunol.* 53:291–325.

Sundberg, J.P. 1994. The balding (bal) mutation, chromosome 18. In Handbook of Mouse Mutations with Skin and Hair Abnormalities: Animal Models and Biomedical Tools. J.P. Sundberg, editor. CRC Press, Boca Raton. 187–191.

Tanaka, T., N.J. Korman, H. Shimizu, R.A.J. Eady, V. Klaus-Kovtun, K. Cehrs, and J.R. Stanley. 1990. Production of rabbit antibodies against carboxy-terminal epitopes encoded by bullous pemphigoid cDNA. *J. Invest. Dermatol.* 94:617–623.

Theis, D.G., P.J. Koch, and W.W. Franke. 1993. Differential synthesis of type 1 and type 2 desmocollin mRNAs in human stratified epithelia. *Int. J. Dev. Biol.* 37:101–110.

Thomas, K.R., C. Deng, and M.R. Capecchi. 1992. High-fidelity gene targeting in embryonic stem cells by using squence replacement vectors. *Mol. Cell. Biol.* 12:2919–2923.

Troyanovsky, S.M., L.G. Eshkind, R.B. Troyanovsky, R.E. Leube, and W.W. Franke. 1993. Contributions of cytoplasmic domains of desmosomal cadherins to desmosome assembly and intermediate filament anchorage. *Cell.* 72:561–574.

Troyanovsky, S.M., R.B. Troyanovsky, L.G. Eshkind, V.A. Krutovskikh, R.E. Leube, and W.W. Franke. 1994. Identification of the plakoglobin-binding domain in desmoglein and its role in plaque assembly and intermediate filament anchorage. *J. Cell Biol.* 127:151–160.

Tybulewicz, V.L.J., C.E. Crawford, P.K. Jackson, R.T. Bronson, and R.C. Mulligan. 1991. Neonatal lethality and lymphopenia in mice with a homozygous disruption of the c-abl proto-oncogene. *Cell.* 65:1153–1163.

Wheeler, G.N., A.E. Parker, C.L. Thomas, P. Ataliotis, D. Poynter, J. Arnemann, A.J. Rutman, S.C. Pidsley, F.M. Watt, D.A. Rees et al. 1991. Desmosomal glycoprotein DGI, a component of intercellular desmosome junctions, is related to the cadherin family of cell adhesion molecules. *Proc. Natl. Acad. Sci. USA.* 88:4796–4800.

Zhang, H., P. Hasty, and A. Bradley. 1994. Targeting frequency for deletion vectors in embryonic stem cells. *Mol. Cell. Biol.* 14:2404–2410.